

## METAL DETECTOR EXCITED BY FREQUENCY-SWEPT SIGNAL

**Jakub Svatoš, Josef Vedral, Pavel Fexa**

CTU in Prague, Faculty of Electrical Engineering, Department of Measurement, Technická 2,166 27, Prague 6, Czech Republic  
(✉ svatoja1@fel.cvut.cz, +420 224 352 201)

### Abstract

This paper describes the theoretical background of electromagnetic induction from metal objects modelling. The response function of a specific case of object shape – a homogenous sphere from ferromagnetic and non-ferromagnetic material is introduced. Experimental data measured by a metal detector excited with a linearly frequency-swept signal are presented. As a testing target various spheres from different materials and sizes were used. These results should lead to better identification of the buried object.

Keywords: Metal detection, Polyharmonic signals, Frequency Sweep, Modelling of electromagnetic induction, Analog signal processing

© 2011 Polish Academy of Sciences. All rights reserved

### 1. Introduction

Land mines, especially Anti-Personnel (AP) mines, are still a worldwide problem. Nowadays a large number of AP mines is buried in the soil (more than sixty million AP mines). These AP mines kill or cripple around 26 thousand people every year. According to the statistics, half of these victims are civilians, mostly children younger than sixteen years of age.

There are many ways to detect AP mines or buried metal objects in general. Currently, electromagnetic manual methods are still major techniques in detection and clearance. Their main disadvantage is that they are very slow due to many false alarms [1], [2]. Reasons for this failure are especially the variety of environments in which the mines are buried and the limits or flaws of current technology [3] and [4]. The excitation signal and signal processing in the detector should be chosen in a way to avoid/minimize false alarms.

### 2. Principles of Metal Detector

Hand held detectors usually consist of a search head which contains primary and secondary coils. When the detector passes over an object able to influence the magnetic field it causes a change in the voltage induced in this coil. The induced voltage generated by the magnetic field represents a complex magnitude because the received signal consists of a signal which is in phase with the transmitted one (in-phase/resistive component) and a signal which is phase-shifted by 90 degrees (quadrature-phase/reactive component). Thus the changes of amplitude and the phase of the received signal contain information about the detected object.

The primary coil is driven by a time-varying electric current  $I_{\text{prim}}$ . This AC current generates a magnetic field  $B_{\text{prim}}$ . This field interacts with the field  $B_{\text{sec}}$  generated by eddy currents induced in detected metallic objects. This can be described by Ampere's Law (1).

$$\oint_1 B dl = \mu_0 I, \quad (1)$$

where  $\mu_0$  is the permeability of vacuum ( $4\pi 10^{-7}$  NA<sup>-2</sup>),  $l$  is the length of a closed curve.

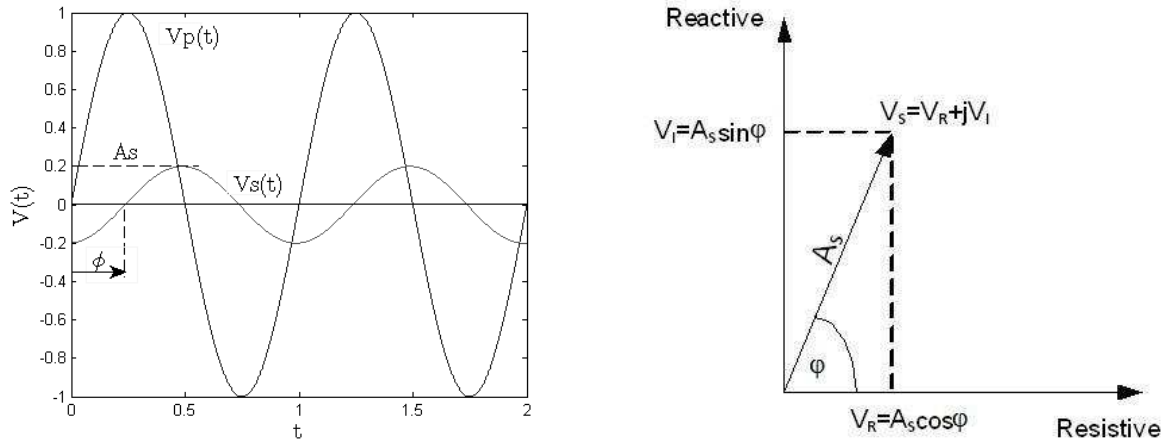


Figure 1: Signal waveform and its phase vector in the complex plane

In accordance with Lenz's law eddy currents generate magnetic fields opposed to the primary field. The secondary magnetic field is detected by the receiver coil(s) and induces an electrical voltage in the receive coil(s) according to the Maxwell-Faraday equation.

$$\oint_1 E dl = - \frac{d\Phi_B}{dt}. \quad (2)$$

where  $E$  is the electric field and  $\Phi_B$  is the magnetic flux.

The equation of the Ampère Law for a circular coil with radius  $a$  can be reformulated using the Biot-Savart Law. This allows to describe the magnetic field at a distance  $d$  along the axis of the coil.

$$B = \oint dB_z = \frac{\mu_0}{4\pi} \oint \frac{Idl \cos \Theta}{a^2}. \quad (3)$$

After solving the Biot-Savart Law one gets the important equation (4) where  $N$  is the number of turns of the coil and  $M$  is magnetic moment  $M = NIS$ .

$$B = \frac{N\mu_0 I}{2} \frac{a^2}{(r^2 + a^2)^{\frac{3}{2}}} = \frac{\mu_0 M}{2\pi(r^2 + a^2)^{\frac{3}{2}}}. \quad (4)$$

From formula (4) is evident that the magnetic field falls off rapidly with the cube of the distance  $d$  from the coil. The secondary magnetic field depends on the distance and orientation of an object, its shape and size, conductivity and permeability but also on the EM background and soil properties. Very important is the frequency of the primary magnetic field as it influences substantially the depth of eddy currents penetration. A low-frequency magnetic field penetrates deeper into the ground, is less affected by the ground effect [5] and also the skin effect is reduced.

On the other hand high frequencies offer better resolution. The dependence of detection properties on the frequency of the exciting electromagnetic field opens the opportunity to develop new methods of primary coil excitation and signal processing of the received signal with the intention to better identify geometry, depth and material of the buried object.

Use of a polyharmonic (non-harmonic) signal offers the chance to obtain more complex information about the buried object. In this way of coil excitation a better outline about the buried object should be acquired in comparison with only single-tone methods.

### 3. Modelling of Electromagnetic Induction from the Target

As described in [6] a simple circuit model could be used for understanding of the behavior of a metal detector with an inductive response. A very simple model consisting of separated transmitting and receiving coils with operating frequency  $\omega$  and a conductive object represented by lumped resistance  $R$  and inductance  $L$  is used as a target. The transmitting coil is driven by current  $I$ . Between any two of these components exists a mutual inductance  $M$ . Construction of these detectors is arranged in a way to have as low mutual inductance as possible when an object is not present. This paragraph also describes possibilities how to distinguish between different objects and identify an object by its characteristic phase response.

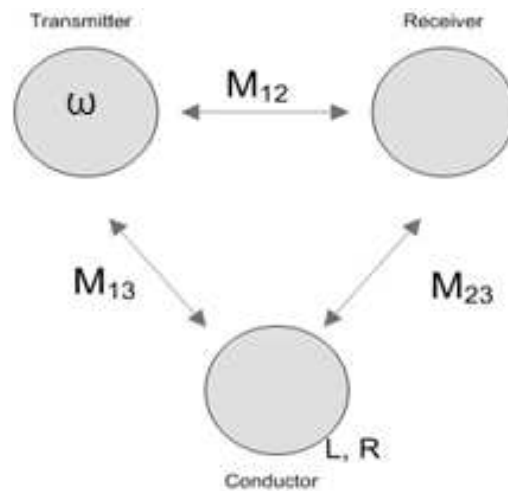


Figure 2: Simple circuit model

The response function for this model is given by formula (5).

$$G(\omega) = -\frac{M_{13}M_{23}}{M_{12}L} \left[ \frac{j\omega L(R - j\omega L)}{R^2 + \omega^2 L^2} \right] = \beta \left[ \frac{\alpha^2 + j\alpha}{1 + \alpha^2} \right]; \quad (5)$$

$$\alpha = \frac{\omega L}{R} \quad \text{and} \quad \beta = -\frac{M_{13}M_{23}}{M_{12}L}. \quad (6)$$

This response  $G(\omega)$  can be rewritten as the product of coupling coefficient  $\beta$ , which depends on the relative size and the position of the component, and response parameter  $\alpha$  which depends on the operating frequency  $\omega$  and  $R$  and  $L$  of the conductor. The coupling coefficient therefore is different for each type of geometry model and must be examined separately. In [6] coefficient  $\alpha$  is rewritten as a response function  $F(\alpha)$  and split into real and imaginary parts. Real parts represent eddy current and hysteresis losses and imaginary parts represent the target's susceptibility.

$$F(\alpha) = \left[ \frac{\alpha^2 + j\alpha}{1 + \alpha^2} \right] = \frac{\alpha^2}{1 + \alpha^2} + j \frac{\alpha}{1 + \alpha^2} = X(\alpha) + jY(\alpha). \quad (7)$$

When  $\alpha$  goes to infinity the real part goes to 1 and the imaginary to 0. This is valid for highly conductive or inductive targets or when operating at high frequencies – this case is called the Inductive limit. On the other hand when  $\alpha$  goes to zero the response function is imaginary and this case is called the resistive limit. The target conductivity is low or the operating frequency is low. When  $\alpha$  is equal to 1 the components are equal to 1/2. Then the phase changes from  $90^\circ$  to  $0^\circ$  as shown in Figure 3. For more information see [1] and [6].

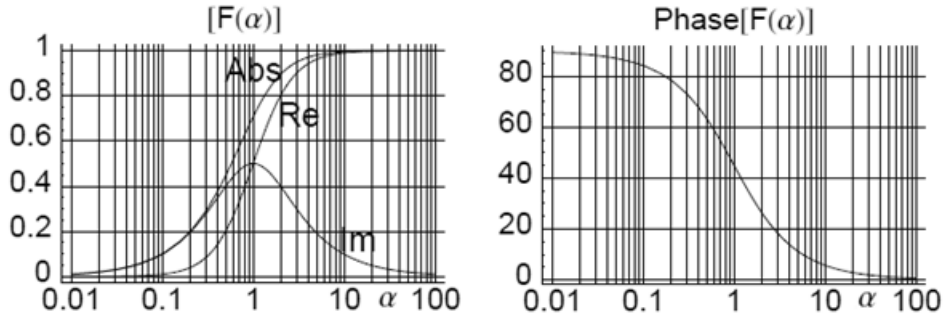


Figure 3: Response function for a simple model [1]

A little bit different is the case of a specific shape of the target – a homogenous sphere. A homogenous sphere represents well an approximation of a common small object. The sphere is in the coil's axis in full space (e.g. infinite external medium). There are many different formulations in literature. Here the formulation from [6] is used.

Having coaxial coils with circular transmitting coil placed in the axis of a homogenous sphere with radius  $a$ , conductivity  $\sigma$  and permeability  $\mu$ , the response  $V_s(8)$  can be determined. The transmitting coil works at operating frequency  $\omega$  and is driven by current  $I$ .

$$V_s = 2\pi j\mu I\omega \frac{R_T^2}{(d_T^2 + R_T^2)} \frac{R_S^2}{(d_S^2 + R_S^2)} (X(ka) + jY(ka)). \quad (8)$$

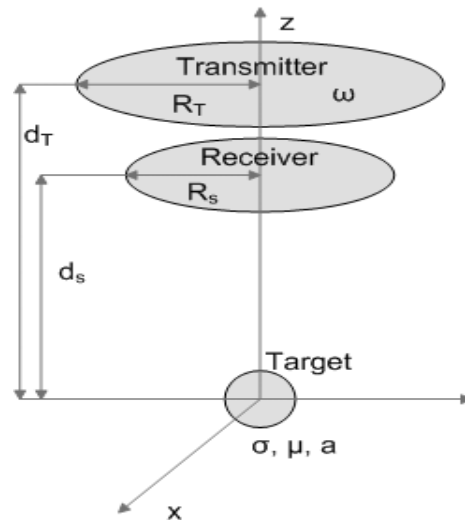


Figure 4: Model of coaxial coils in the axis of a homogenous sphere

Term  $\chi_n(ka)$  depends on the frequency as well as on target properties and it is similar to the Response Function  $F(\alpha)$  from simple modelling. The response parameter  $\alpha$  is now

$$k^2 a^2 = j\omega\mu\sigma^2 = j\alpha. \quad (9)$$

The variable  $\alpha$  is purely imaginary and depends on object parameters (also on depth of penetration). If the coil is at a larger distance from the sphere or the sphere is much smaller than the diameter of coils, the sphere acts like a magnetic dipole and only the first term is relevant. A magnetic dipole has a magnetic moment which is always aligned with the transmit field  $H_{\text{prim}}$ . The phase response also depends on objects electromagnetic parameters and frequency but not on its geometry.

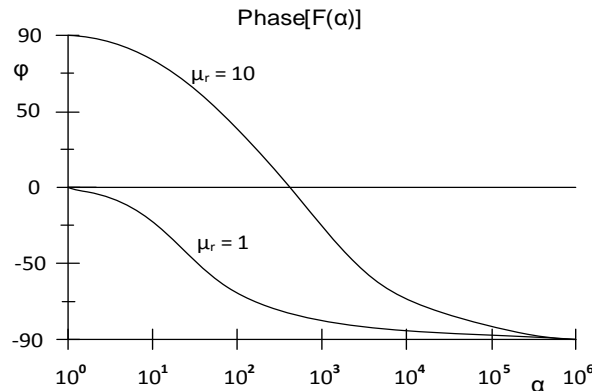


Figure 5: Response function of ferromagnetic ( $\mu_r = 10$ ) and non-ferromagnetic ( $\mu_r = 1$ ) object

Focused on a non-ferromagnetic object ( $\mu_r = 1$ ), the response function and its plot is quantitatively similar to simple circuit model (Fig. 3). The response function for ferromagnetic material in dipole approximation is a little bit different. Looking at phases in Figure 5 it is clear that only ferromagnetic objects have a positive phase response but if  $\alpha$  is going to infinity the phase goes to  $-90^\circ$  for both non-ferromagnetic and ferromagnetic objects. Focusing to recognize if the object (with negative phase response) is ferromagnetic or not, multiple frequencies must be used.

According to this model and its response function using polyharmonic signals, the whole or at least part of the frequency characteristic of the object will be given. Based on this characteristic more details about the buried object could be examined.

### 3. Experimental Data

All the experimental data are measured in laboratory conditions by metal detector Schiebel ATMID – (All Terrain Mine Detector).

A searching head with a diameter of 267 mm and an non-typical setup of transmitting and receiving coils is used in this metal detector. The ATMID detector has partially overlapped transmitting and receiving coils (Fig 6 – right). The coil is excited using a polyharmonic frequency-swept signal (Fig. 7) defined by equation (10). The range of frequencies is bounded from bottom by the level of the received signal (2) and by the skin effect from the top.

$$x(t) = \sin \left[ 2\pi \left( f_0 + \frac{k}{2} t \right) t \right], \quad (10)$$

where  $f_0$  is the start frequency,  $t$  is sweep time and  $k$  is the sweep rate.

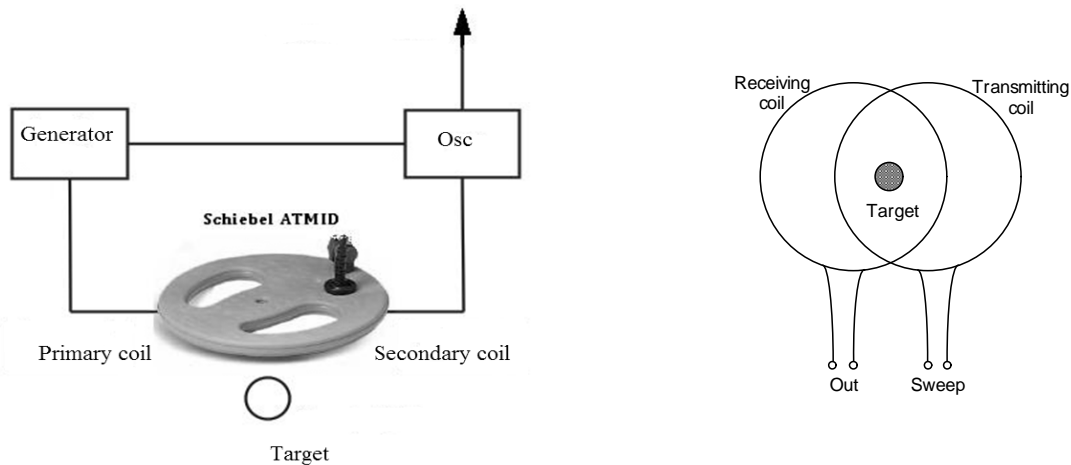


Figure 6: Blok diagram of a workplace (left) and coil setup of the searching head (right)

For the measurement a linear frequency sweep from 1 kHz to 50 kHz is used with a time sweep of 10 ms. The frequency range used is below the resonant frequency of the coil (90 kHz). Excitation and received signal is measured with a MSO 4034 oscilloscope in hi-res mode with a sampling frequency of 500 MSample/s.

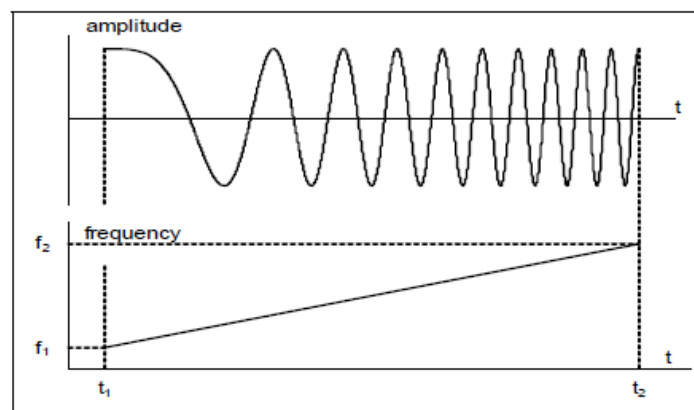


Figure 7: Linear frequency sweep [7]

Small spheres from different materials and sizes and a true grenade without the explosives (Fig. 12 - left) are used as targets. Tested objects are placed 50 mm from the coil in the middle of the searching head in open air (Fig. 6 – right). The spheres are placed so close in order to avoid interference of laboratory equipment (the received signal is very low).

An example of the received signal is shown in Figure 8. Measured data were processed in MATLAB. The amplitude and phase spectra are done as well as Power Spectral Density - Periodograms.

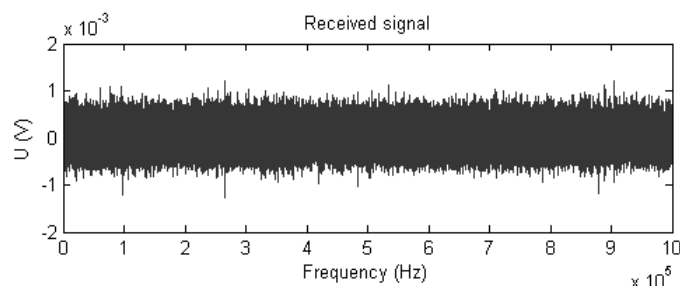


Figure 8: Sample of the received signal (bronze 10mm)

Spectra are computed from 1M points ( $2^{20}$  using zeros padding) and the Blackman-Harris window was used. Amplitude and phase spectra of two samples (bronze and UNI100Cr6) are presented in Figure 9. Uni100Cr6 is a material used for testing and calibration of metal detectors. By this way of signal excitation, more information about the buried object is obtained in comparison with using only one frequency.

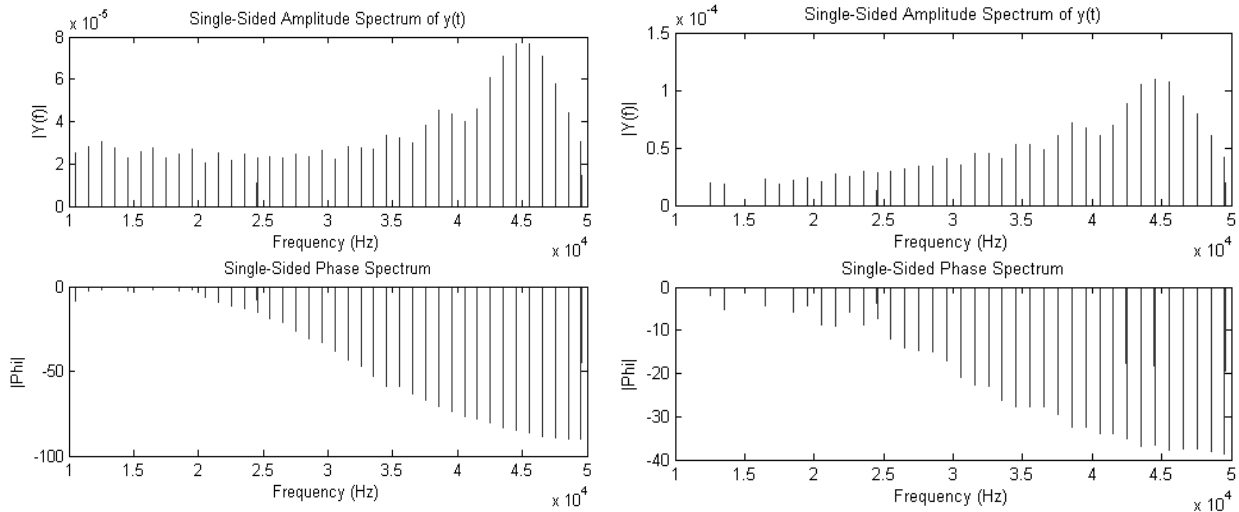


Figure 9: Amplitude and phase spectra of bronze 10mm (left) and UNI100Cr6 10mm (right)

The phase spectrum of the bronze object corresponds to theory and inductive and resistive limits of the object are evident. The frequency covers the entire response function. On the other hand, the phase spectrum of the UNI100Cr6 (same size) changes only in a range of 50 degrees. The same case is for the phase spectrum of the grenade (Fig. 12 – right). For this range of the sweep signal it is not possible to reach the whole response function (inductive and/or resistive limit). For better data interpretation a polar graph can be shown (Fig. 10).

As shown in Figures 11 (right) and 12 (right) it is not possible to distinguish between INOX and grenade if only one frequency between 10 kHz – 15 kHz is used. It is so because the phase shift in the frequency band is identical. The amplitude spectrum is different but it could be due to the distance from detector. In this way of excitation, differentiation between two objects (INOX and grenade) is not possible. On the other hand in the frequency band 15 kHz to 50 kHz the phase spectrum is different and difference between objects can be shown. See Figure 13.

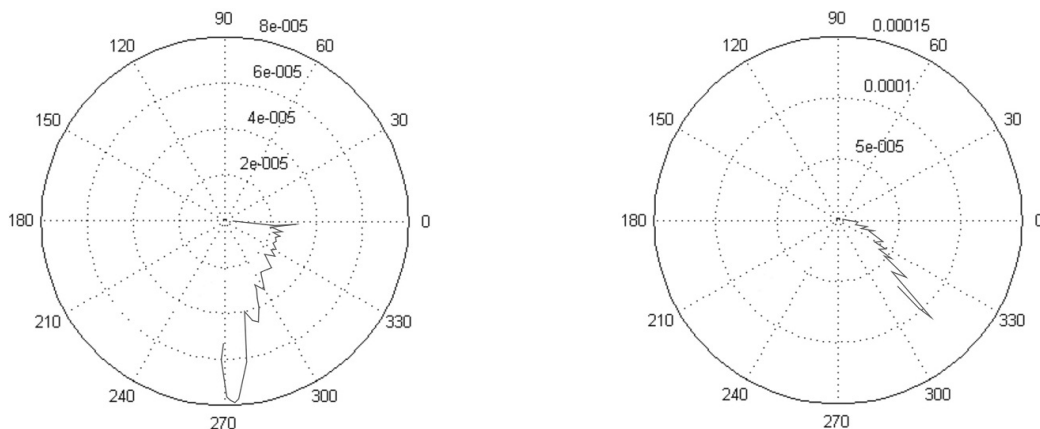


Figure 10: Polar graph of bronze 10mm (left) and UNI100Cr6 10mm (right)

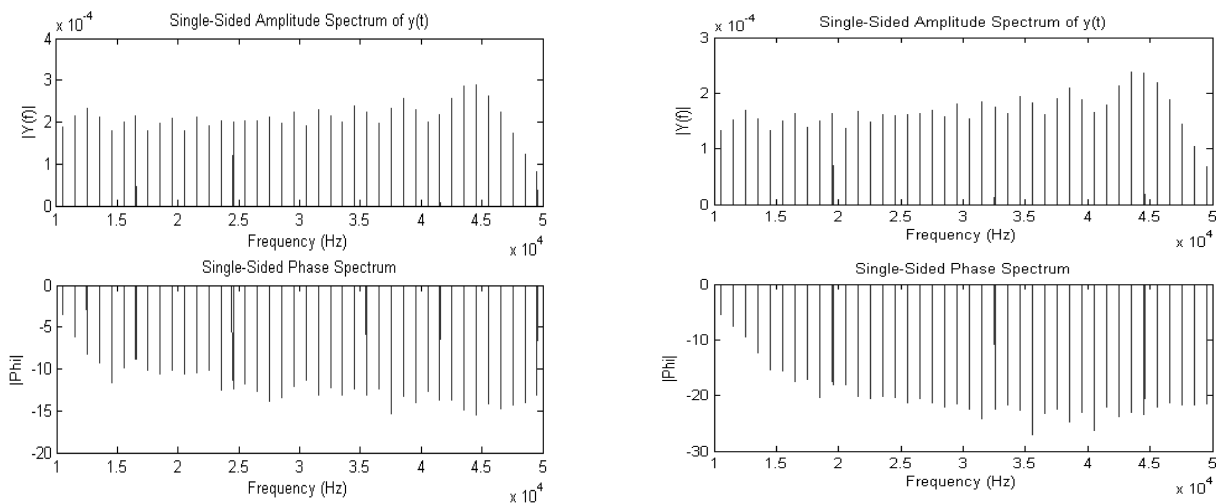


Figure 11: Amplitude and phase spectra of brass 10mm (left) and INOX 10mm (right)

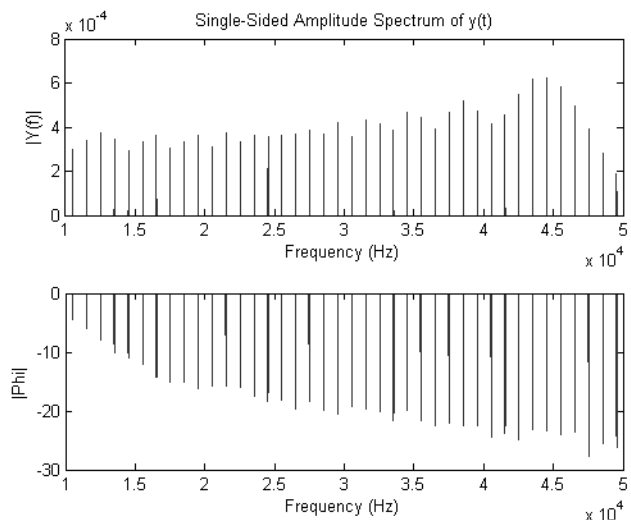
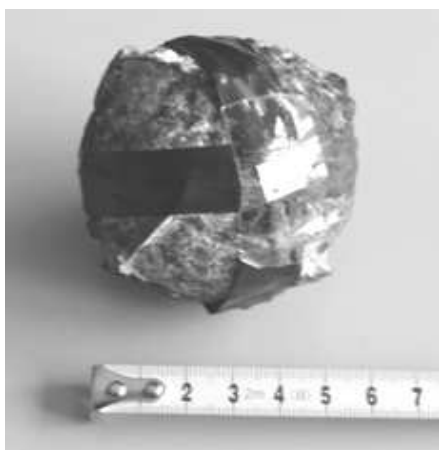


Figure 12: Photo of the grenade (left) and amplitude and phase spectra of grenade (right)

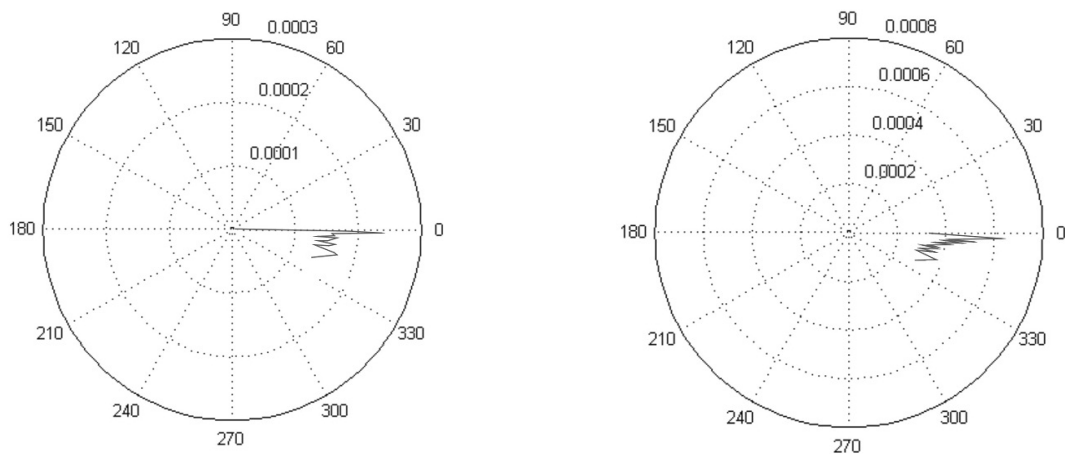


Figure 13: Polar graph of the grenade (left) and INOX 10mm (right)

On the basis of these measurements, the detector can be calibrated for a specific object by means of a classifier. In this way, the detector will be sensitive to the specific object (for example an AP mine).

Another possible method how to take advantage of sweep is signal processing using power spectral density. In Figure 14 are Periodograms for different sizes and materials of targets. A PSD relative to frequency could provide additional information about a buried object. This method is not effective in the recognition of the target's material but could bring more information about its size thanks to the level and shape of the signal. Future research should disclose if it is possible to differentiate a bigger object from multiple small objects using the PSD method.

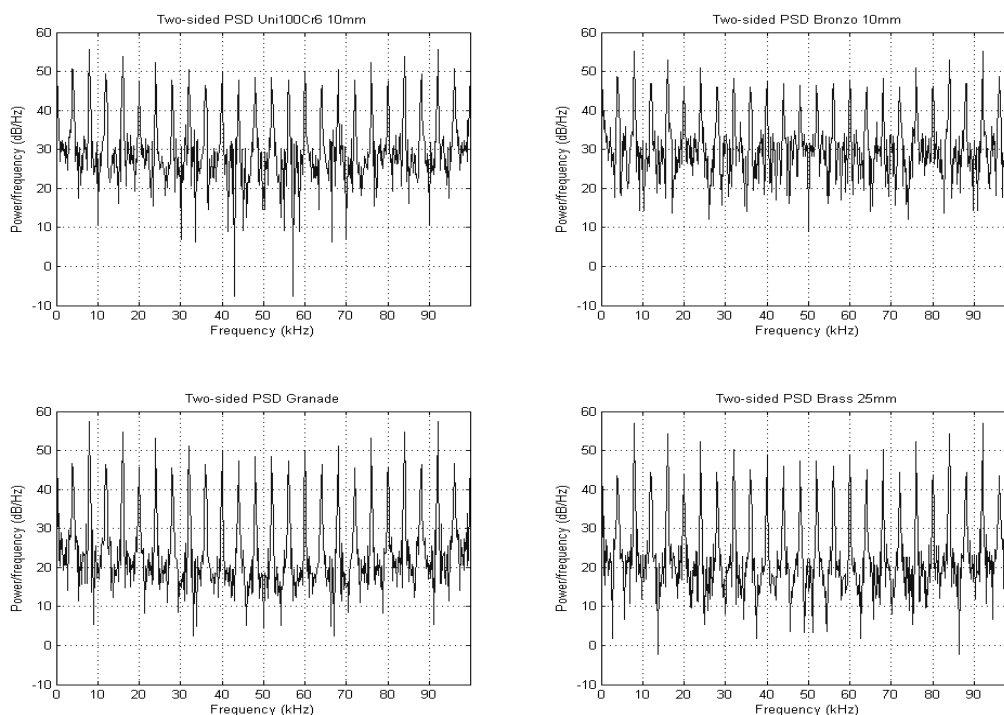


Figure 14: Periodograms for different sizes and materials of the targets

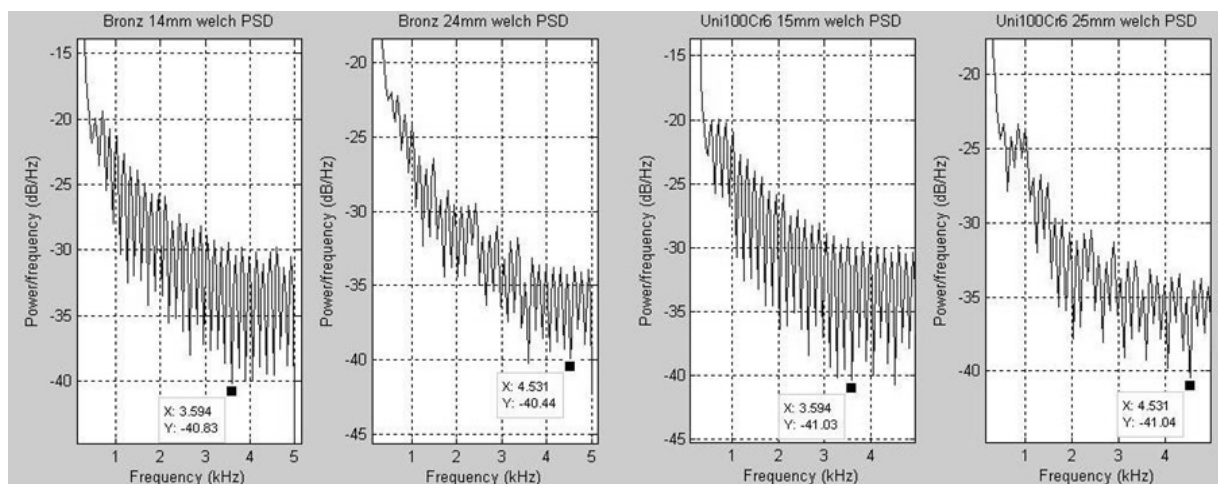


Figure 15: Detail (1-5 kHz) of Welch's method Periodograms for different sizes and materials of the targets

Last method used is PSD using the Welsch method. As shown in Figure 15, a signal processed using this method confirms the conformity of different material but the same size. Power distribution due to the frequency may help to identify the real size of metal objects. These methods offer significant opportunities in the processing of signals from the metal detectors excited by polyharmonic signals.

#### 4. Conclusions

In this article the analysis of the electromagnetic induction response function for the simple model and homogenous sphere was presented, as well as measured experimental data from different objects. For data processing FFT and PSD methods were used. Based on this analysis it is evident that a better outline of the object in terms of geometric and electromagnetic (conductivity, permeability) properties can be obtained when the excitation of the detector is done by multiharmonic signal – linear frequency sweep. Using multiharmonic signals results in more complex information about buried objects thanks to their response function. To identify an object the well known method of amplitude and phase response determination and also Periodograms are used. PSD should improve identification of the object in combination with the FFT method. Further investigation will be focused on the research using different multi-frequency signals (AM, FM and  $\sin x/x$  signals) as the excitation signal and other signal processing (Wavelet transform) [8]. Another interesting area which needs to be focused in future is using different soil instead of open air as the surrounding medium [9].

#### Acknowledgements

This project is supported by the research program No. 102/09/H082 “Sensors and Intelligent Sensors Systems” of the CTU in Prague, sponsored by the Czech Science Foundation and the grant SGS 10/207/OHK3/2T/13” Digitization, synchronization and signal processing in sensors and sensor networks” by the Grant Agency of the Czech Technical University in Prague.

#### References

- [1] Brooks, J.W. (2000). *The Detection of Buried Non-Metallic Anti-Personnel Land Mines*. The University of Alabama in Huntsville. Huntsville. Alabama.
- [2] Azevedo, S.G., Stull S. (1997). Making Land-Mine Detection and Removal Practical. <https://www.llnl.gov/str/Azevedo.html>.
- [3] Riggs, L.S., Mooney, J.E., et al. (1998). Identification of Metallic Mines using Low Frequency Magnetic Fields, in Proc. *SPIE Int. Detection and Remediation Technologies for Mines and Minelike Targets III*. Orlando, FL, 146–157.
- [4] Composite Authors (2002). Project Mimeva, Study of Generic Mine-Like Objects for R&D in Systems for Humanitarian Demining – Final Report. Ispra.
- [5] Bruschini, C. (August 2004). On the Low Frequency EMI Response of Coincident Loops Over a Conductive and Permeable Soil and Corresponding Background Reduction Schemes. *IEEE Trans. Geosci. Remote Sens.*, 42(8), 1706–1719.
- [6] Bruschini, C. (2002). *A Multidisciplinary Analysis of Frequency Domain Metal Detectors for Humanitarian Demining*. Vrije Universiteit Brussel. Brussel.
- [7] Vedral, J., Svatoš, J., Fexa, P. (2009). Methods for Economical Test of Dynamic Parameters ADCs. *Metrology and Measurement Systems*, 16(1), 161-170.

- [8] Adamczak, S., Makiela, W., Stepień, K. (2010). Investigating Advantages and Disadvantages of the Analysis of a Geometrical Surface Structure with the Use of Fourier and Wavelet Transform. *Metrology and Measurement Systems*, 17(2), 233–244.
- [9] (2002). International Test and Evaluation Program for Humanitarian Demining, Soil Electromagnetic Characteristics and Metal Detector Performance, European Commission Joint Research Centre Via E. Fermi. Ispra.